

# Immobilized Lipase Based on Hollow Mesoporous Silicon Spheres for Efficient Enzymatic Synthesis of Resveratrol Ester Derivatives

Liu-Jia Xu,<sup>#</sup> Tao Yang,<sup>#</sup> Jing Wang, Feng-Hong Huang, and Ming-Ming Zheng\*



Cite This: <https://dx.doi.org/10.1021/acs.jafc.0c07501>



Read Online

ACCESS |



Metrics & More



Article Recommendations



Supporting Information

**ABSTRACT:** Enzymatic esterification of resveratrol is crucial for its potential application in lipophilic foods and drugs. However, the poor activity of the free enzyme hinders the reaction. In this work, the highly efficient enzymatic synthesis of resveratrol ester derivatives was achieved by immobilized lipase on hydrophobic modified hollow mesoporous silicon spheres (HMSS-C<sub>8</sub>). We preliminarily explored the use of *Candida* sp. 99-125 lipase (CSL) for the acylation of resveratrol, with a regioselectivity toward 3-OH- over 4'-OH-acylation. HMSS-C<sub>8</sub> provided ideal accommodation for CSL with a loading capacity of up to 652 mg/g. The catalytic efficiency of CSL@HMSS-C<sub>8</sub> was 15 times higher than that of free CSL, and the conversion of resveratrol reached 98.7% within only 2 h, which is the fastest value recorded in the current literature. After 10 cycles, the conversion remained up to 86.3%. Benefiting from better lipid solubility, the relative oxidation stability index values of oil containing monoester derivatives were 43.1%–68.8% and 23.9%–33.2% higher than that of refined oil and oil containing resveratrol, respectively. This research provides a new pathway for efficient enzymatic synthesis of resveratrol ester derivatives and demonstrates the potential application of resveratrol monoester derivatives as a group of excellent lipid-soluble antioxidants.

**KEYWORDS:** resveratrol, regioselectivity, immobilized lipase, antioxidant, enzymatic synthesis

## INTRODUCTION

Resveratrol (3-4'-5-trihydroxystilbene), also known as phytoalexin, is a nonflavonoid polyphenol compound mainly distributed in grapes, berries, peanuts, and other plants. It has been reported that resveratrol exhibits numerous bioactivities, including antioxidant,<sup>1</sup> anti-inflammatory,<sup>2</sup> anti-tumor,<sup>3</sup> antiobesity,<sup>4</sup> protection of cardiovascular,<sup>5</sup> and nervous system.<sup>6</sup> However, the poor stability and solubility impeded its applications in the fields of food and medicine severely. Moreover, related metabolic studies have shown that resveratrol exerts a poor bioavailability,<sup>7–9</sup> implying limited biofunction even after ingestion. Thus, esterification modification has been carried out for increasing lipophilicity, higher stability, and bioavailability.<sup>10–12</sup> There are two esterification sites of resveratrol, i.e., 3-OH and 4'-OH. It has been reported that esterification at 3-OH can prevent resveratrol from being converted into 3-sulfate and 3-glucuronide derivatives in the metabolism of the liver, thereby improving its bioavailability.<sup>13</sup> Esterification at the 4'-OH can increase the stability of resveratrol without reducing its antioxidant activity.<sup>14</sup>

Esterification via a chemical process usually faces several drawbacks such as nonregioselectivity, undesirable byproduct, and environmental damage.<sup>15</sup> From this aspect, enzymatic synthesis has gradually become the trend in the field of catalysis contributing to the high regioselectivity,<sup>16</sup> mild reaction conditions,<sup>17</sup> and environmental protection.<sup>18</sup> Among the family of enzymes, lipase (triacylglycerol ester hydrolases, EC 3.1.1.3) is indispensable owing to the remarkable catalytic performance in hydrolysis,<sup>19</sup> esterification,<sup>20</sup> transesterification,<sup>21</sup> and alcoholysis.<sup>22</sup> Previous studies have reported the lipase-catalyzed synthesis of resveratrol ester

derivatives, but it was generally conducted with long reaction time but low yield.<sup>23,24</sup> Torres *et al.*<sup>14</sup> selected Lipase QL<sub>G</sub> to catalyze the esterification of resveratrol in 2-methyl-2-butanol for up to 160 h, which may be due to the low catalytic activity of lipase in the organic solvent with strong polarity. In general, free lipases are limited by vulnerable activity, inferior stability, and reusability.<sup>25</sup> In contrast, properly immobilized lipase displayed enhanced stability in harsh environments, which could be effectively recycled further.<sup>26</sup> Therefore, lipase immobilization is particularly crucial for synthesis of resveratrol derivatives in the food and pharmaceutical industries.

To date, various carriers have been utilized for enzyme immobilization, including mesoporous materials,<sup>27</sup> carbon nanomaterials,<sup>28</sup> magnetic particles,<sup>29</sup> metal–organic frameworks,<sup>30</sup> and covalent organic frameworks.<sup>31</sup> Among the various possible immobilized carriers, hollow mesoporous silicon spheres (HMSS) were featured with a large surface area, controllable pore structure, and narrow pore size distribution, which provide sufficient space and ideal accommodation for lipases.<sup>27</sup> Besides, it is chemically and mechanically stable and can be chemically modified with various functional groups.<sup>32,33</sup> These characteristics made HMSS an attractive material for lipase immobilization. However, the multitudinous hydrophilic hydroxyl groups on the surface of the silicon material were

**Special Issue:** Lipid Science and Health

**Received:** November 27, 2020

**Revised:** January 31, 2021

**Accepted:** February 3, 2021



unfavorable for exposure of active sites and would hinder the activity of lipases. In general, the "lid" structure is rearranged in the hydrophobic environment to uncover the catalytic triad, then the substrate has a chance to enter the interior and come into contact with the active center.<sup>17</sup> Therefore, the immobilization of lipase on the hydrophobic carriers is preferable. Taking this into consideration, it is a promising strategy to immobilize lipase on the hydrophobic modified HMSS for enzymatic esterification of resveratrol.

In this work, the enzymatic preparation of resveratrol ester derivatives was successfully achieved by immobilizing lipase on hydrophobic modified hollow mesoporous silica spheres. Compared with free lipase, immobilized lipase showed superior catalytic activity and reusability. The content of monoesters and diester in the product could be regulated by adjusting reaction conditions. In addition, monoester derivatives showed higher antioxidant activity than resveratrol. This study holds great promise for expanding the application of resveratrol in food, medicine, cosmetics, and other fields.

## MATERIALS AND METHODS

**Materials.** Resveratrol (98%) was purchased from Xi'an Four Seasons Biotechnology Co. Ltd. Linseed oil, soybean oil, rapeseed oil, and peanut oil were all refined without any antioxidants purchased from supermarkets. Lipase AYS (*Candida rugosa*, lyophilized powder), Lipase DF (*Rhizopus oryzae*, lyophilized powder), Lipase PS (*Burkholderia cepacia*, lyophilized powder), and Lipase CRL (*Candida rugosa*, lyophilized powder) were purchased from Amano Enzyme Inc. Lipase CSL (*Candida* sp. 99-125, lyophilized powder) was purchased from Beijing Kaitai New Century Biotechnology Co. Ltd. Lipozyme RM IM and Novozym 435 were purchased from Novozymes (China) Biotechnology Co. Ltd. Enhanced (BCA) Protein Assay Kit was obtained from Shanghai Yuan Ye biotechnology. Cetyltrimethylammonium bromide (CTAB) and silane coupling agent ( $C_8$ -TEOS) were purchased from Sigma-Aldrich (St. Louis, MO). Vinyl octyl and vinyl laurate were purchased from Tixiai Chemical Industrial Development Co. Ltd. Toluene, sodium metasilicate nonahydrate ( $Na_2SiO_3 \cdot 9H_2O$ ), 2-methyl-2-butanol (2M2B), methyl *tert*-butyl ether (MTBE), vinyl acetate, and other chemicals were supplied by Sinopharm Chemical Reagent (Shanghai, China) and were of analytical reagent grade.

**Synthesis of HMSS and HMSS- $C_8$ .** HMSS was prepared and purified according to previously reported methods.<sup>34</sup> A 39.0 g sample of CTAB and 46.0 g of solid  $Na_2SiO_3 \cdot 9H_2O$  were added into 700 mL of purified water, and the solution was stirred vigorously at 30 °C until the solution became clear. Subsequently, 75 mL of ethyl acetate was quickly added in, and the mixture was stirred for 30 s. After standing at 30 °C for 5 h, the mixture was aged at 90 °C for 48 h. Then, the solid products were filtered and dried at room temperature. Finally, the dried HMSS was calcined at 550 °C for 5 h in the muffle furnace and stored dry for further use. At the next stage, HMSS particles were modified by silane coupling agent ( $C_8$ -TEOS) grafting on the HMSS surface. A 1.0 g sample of HMSS, 1.3 g of  $C_8$ -TEOS, and 15  $\mu$ L triethylamine were added to 10 mL of toluene. Subsequently, the mixture was placed in a Teflon-lined stainless-steel autoclave and reacted in an oven (130 °C) for 20 h. The white precipitate was collected by centrifugation (2990g, 10 min), then washed several times with ethanol, and dried in a vacuum oven (60 °C). The modified hollow mesoporous silicon spheres (HMSS- $C_8$ ) were obtained.

**Immobilization of CSL on HMSS- $C_8$ .** First, lipase CSL was added to phosphate buffer (50 mM), and the lipase suspension was stirred at 4 °C for 15 min at 200 rpm and then centrifuged (2990g, 10 min) to obtain a certain concentration of lipase solution. Subsequently, 0.1 g of HMSS- $C_8$  (presoaked with 200  $\mu$ L ethanol) was added to the 8 mL of lipase solution and mixed by shaking. After being vacuumized for 5 min, the mixture was shaken for 30 min (20

°C, 200 rpm) and then centrifuged (2990g, 10 min). The supernatant was collected to assay the amount of residual protein concentration by a BCA protein assay, and the precipitate (CSL@HMSS- $C_8$ ) was washed three times with phosphate buffer and freeze-dried.

**Characterization of HMSS, HMSS- $C_8$ , and CSL@HMSS- $C_8$ .** The surface morphologies of the samples were observed by scanning electron microscopy (SEM; SU8010, Hitachi, Tokyo, Japan) at 200 kV. Before the test, the sample was dispersed in absolute ethanol for 10 min. After the ethanol evaporated, it was dispersed on the SEM copper net for observation. The Brunauer–Emmett–Teller (BET) surface area and the total pore volume were measured with a computer-controlled nitrogen gas adsorption analyzer (ASAP2010) in the relative pressure range of 0.05–1.00. Fourier transform infrared (FT-IR) spectra were recorded on a TENSOR 27 FTIR spectrometer (Bruker, Karlsruhe, Germany). Elemental analysis was performed on an elemental analyzer (Vario EL cube, Elementar, Germany).

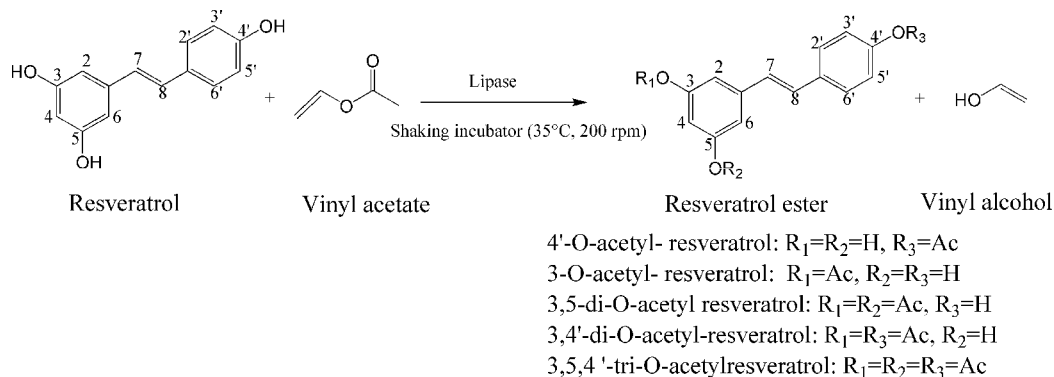
**Enzymatic Synthesis of Resveratrol Ester Derivatives.** For the enzyme screening, the enzymatic reaction was conducted as follows: resveratrol (0.1 g) and vinyl acetate (1.8 g) were added to solvent (5 mL) and dissolved with stirring at 40 °C. Subsequently, enzyme (0.2 g) was added, and the mixture was placed in a shaking incubator (40 °C, 200 rpm) to react for 48 h. For the reaction of different acyl donors and resveratrol, resveratrol (50 mM) and acyl donor (750 mM) were added to 5 mL of MTBE and dissolved with stirring at 35 °C. Subsequently, 0.1 g of free CSL or CSL@HMSS- $C_8$  was added and placed in a shaking incubator (35 °C, 200 rpm) to react. In order to investigate the effect of immobilization on the catalytic capacity of lipase, the reaction catalyzed by immobilized lipase was conducted as follows: resveratrol (50 mM) and vinyl acetate (750 mM) were added to 5 mL of MTBE and dissolved with stirring at 35 °C. Subsequently, 0.1 g of immobilized lipase was added, and the mixture was placed in a shaking incubator (35 °C, 200 rpm) to react. A 100  $\mu$ L sample solution from each reaction process was taken at regular intervals and diluted with chromatographic grade methanol. The obtained sample was filtered by 0.22  $\mu$ m PDVF filters and analyzed by high-performance liquid chromatography (HPLC).

**Purification of Resveratrol Ester Derivatives.** The acetylated resveratrol derivatives were purified using column chromatography on silica gel. The solvent was *n*-hexane/ethyl acetate (5:4, v/v). Each fraction was collected and monitored by TLC (*n*-hexane/ethyl acetate/acetic acid, 10:8:1, v/v/v). Each purified compound was obtained following solvent removal by rotary evaporation.

**Identification of Resveratrol Derivatives.** The content of resveratrol esters was monitored by an HPLC system (LC-20AD, Shimadzu, Japan) equipped with a photodiode array (PDA) detector. The column was a Venusil MP C18 reverse-phase chromatography column (5  $\mu$ m, 4.6  $\times$  250 mm). The mobile phase was methanol/0.1% acetic acid in water (60:40, v/v). The acylated products of resveratrol were quantified by measuring the absorbance at 310 nm. The column temperature was 40 °C, and the flow rate was 1.0 mL/min. The injection volume was 10  $\mu$ L. The chemical structures of resveratrol derivatives were analyzed by an HPLC instrument (LC-40D, Shimadzu, Japan) coupled to a mass spectrometer (LCMS-8050, Shimadzu, Japan). Chromatographic conditions were as described above, except the flow rate was lowered to 0.7 mL/min. Ionization was performed by atmospheric pressure chemical ionization (APCI), and the mass spectrometer detector was a triple quadrupole combination. The pure compounds were obtained by preparative chromatography (LC-6AD, Shimadzu, Japan). Proton nuclear magnetic resonance (<sup>1</sup>H NMR, Bruker, 400M) spectroscopy was performed to identify their molecular structures (400 MHz, DMSO-*d*<sub>6</sub> or CDCl<sub>3</sub>).

**Determination of Antioxidant Activity.** Accelerated oxidation tests were carried out on linseed oil, soybean oil, rapeseed oil, and peanut oil by Rancimat (Model 743, Herison, Switzerland). First, the oil samples were prepared as follows: the amount of resveratrol, monoesters (mixture of 4'-O-acetyl-resveratrol and 3-O-acetyl-resveratrol) and diester (3,5-di-O-acetyl-resveratrol) added in each oil was 0.2 g/kg. The refined oil without any addition was taken as the control. Then, 3.0 g of oil samples were heated at 110 °C under

## Scheme 1. Acetylation of Resveratrol with Vinyl Acetate



purified air, at a flow rate of 20 L/h. The induction times of the tested samples were recorded and used as their oxidative stability index. The measurement was repeated three times for each sample.

## RESULTS AND DISCUSSION

**Enzyme Screening.** In the lipase-catalyzed reaction, different lipases possess varied biochemical properties and catalytic characteristics; thus, lipase selection is vital for directional and efficient catalysis. In this study, resveratrol acetyl esters at different esterification sites were obtained by lipase-catalyzed transesterification of resveratrol with vinyl acetate. The reaction mechanism is shown in Scheme 1. Several lipases (lipase AYS, lipase DF, lipase PS, lipase CRL, lipase CSL, lipozyme RM IM, and Nov435) were selected to investigate the enzymatic synthesis of resveratrol acetyl ester in different solvents. For higher solubility of resveratrol and lipase activity, the solvents (2M2B and MTBE) were selected according to previous reports.<sup>16,35</sup> As shown in Figure 1, among the lipases, the catalytic activity of lipase CSL was higher than that of others, and the catalytic activity of all lipases in MTBE were higher than that in 2M2B. In particular, the resveratrol was almost completely converted by the lipase CSL in MTBE, but the conversion in 2M2B was only 50%.

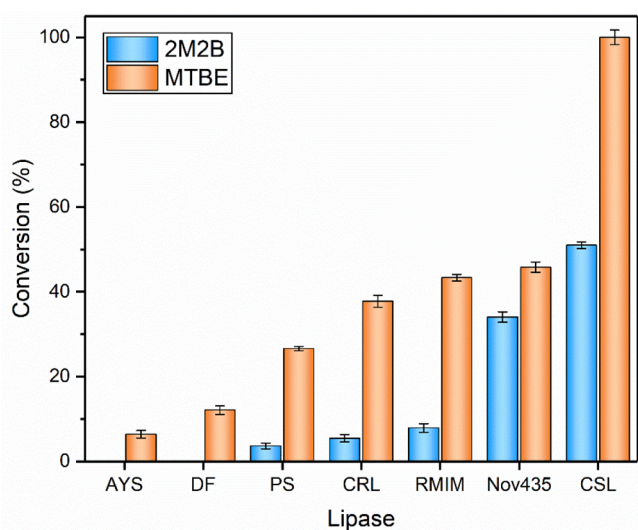


**Figure 1.** Effects of enzymes and solvents on the conversion of resveratrol. Reactions were carried out in solvent (5 mL) containing resveratrol (0.1 g), vinyl acetate (1.8 g), and enzyme (0.2 g) in a shaking incubator (40 °C, 200 rpm) for 48 h.

This result was similar to that reported by Wang *et al.*<sup>16</sup> The higher catalytic activity of lipase in MTBE may be related to the polarity of solvent, because the lipases were reported to be more active and stable in hydrophobic organic solvents with lower polarity.<sup>36,37</sup> Therefore, lipase CSL and MTBE were selected for further study.

**Characterization of HMSS, HMSS-C<sub>8</sub>, and CSL@HMSS-C<sub>8</sub>.** The surface morphologies of HMSS were characterized by scanning electron microscopy (SEM). As shown in Figure 2a, HMSS presented a monodisperse, uniform, and spherical morphology with an average diameter of about 3.4 μm. After being crushed by high-pressure, the hollow structure of the HMSS could be observed clearly (Figure 2b). Also, the BET method was applied to further demonstrate the mesoporous structure of the samples. As shown in Figure 2c,d, the nitrogen adsorption–desorption isotherm showed typical type IV and H<sub>1</sub> isotherm patterns, and the pore width of HMSS and HMSS-C<sub>8</sub> were about 13 nm, which permits lipase CSL (5.0 × 4.2 × 3.3 nm<sup>3</sup>) to enter the cavity of HMSS. As listed in Table 1, the pore volume and surface area of HMSS-C<sub>8</sub> were slightly smaller than those of HMSS, which indicated that C<sub>8</sub> was grafted on HMSS surface successfully. It should be noted that the pore size was not affected apparently, so the modification of C<sub>8</sub> might not hinder the lipase entry into the cavity of HMSS. As suggested by the above results, HMSS-C<sub>8</sub> could be an ideal candidate for lipase immobilization.

In order to verify that C<sub>8</sub> was grafted on the surface of HMSS and lipase CSL was immobilized on the HMSS-C<sub>8</sub>, Fourier transform infrared (FT-IR) spectroscopy was carried out to characterize the structure of materials and immobilized lipase. As shown in Figure 3, typical peaks at 2921 and 2862 cm<sup>-1</sup> corresponded to the symmetric and asymmetric stretching vibration of C–H, suggesting that the C<sub>8</sub> was grafted to HMSS. Besides, the peak at 1544 cm<sup>-1</sup> could be assigned to the N–H bending vibration in the spectra of CSL and CSL@HMSS-C<sub>8</sub>, indicating that lipase CSL was immobilized on HMSS-C<sub>8</sub> successfully. Combustion elemental analysis was employed for systematic analysis of HMSS-C<sub>8</sub> to further determine the grafting degree of C<sub>8</sub> (Table S1), and the grafting degree of C<sub>8</sub> was calculated to be 1.77 mmol/g according to the content of C element.

**Optimization of Immobilization Conditions.** It is well-accepted that buffer pH and initial protein concentration of lipase are critical parameters for the immobilization. In the organic solvent system, the environment of the enzyme relies on the pH of buffer solution before lyophilization or adsorption on the carrier.<sup>38,39</sup> As shown in Figure 4a, both

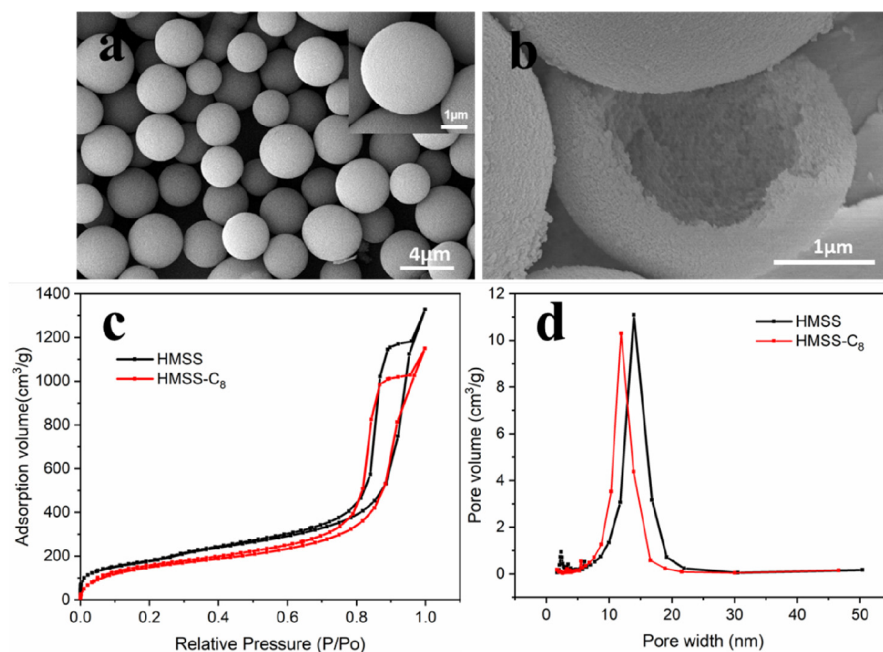


**Figure 2.** SEM images of HMSS (a and b).  $N_2$  adsorption–desorption isotherms (c) and pore size distribution curves (d) of HMSS and HMSS- $C_8$ .

**Table 1.** Textual Parameters of HMSS and HMSS- $C_8$

| sample      | surface area ( $m^2/g$ ) | pore volume ( $cm^3/g$ ) | pore size (nm) |
|-------------|--------------------------|--------------------------|----------------|
| HMSS        | 639                      | 2.05                     | 12.8           |
| HMSS- $C_8$ | 560                      | 1.78                     | 12.7           |

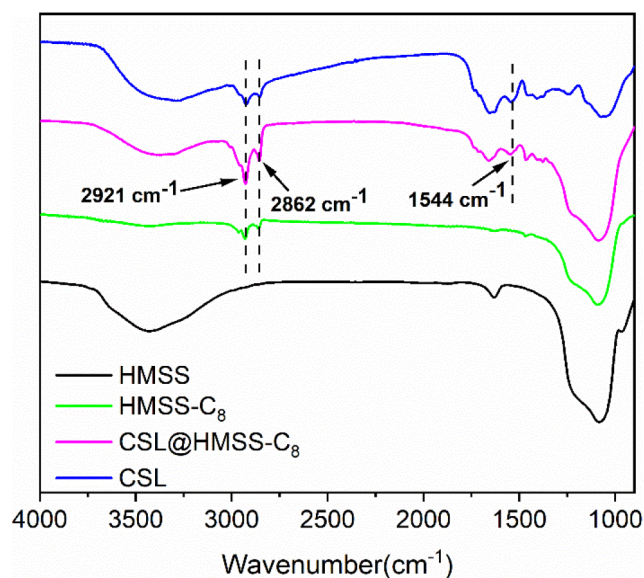


**Figure 3.** FT-IR spectra of HMSS, HMSS- $C_8$ , CSL, and CSL@HMSS- $C_8$ .

the loading amount and conversion of resveratrol increased gradually with the increasing pH and reached their maxima at pH 8.5. However, at pH 5–6, the reaction hardly proceeded despite the loading amount reaching 146–172 mg/g. According to the study reported by Gao *et al.*,<sup>40</sup> it can be inferred that pH 8.5 was around the optimum pH range for lipase CSL activity. Nevertheless, at pH 5–6, the conformation of lipase may be changed, leading to reduced activity and even inactivation of lipase.<sup>41</sup> Therefore, the optimum pH value of

the buffer solution was 8.5, and the acidic conditions were not conducive to immobilized lipase CSL.

The initial protein concentrations of lipase solutions ranging from 2 to 24 mg/mL were prepared, and their effect on immobilization was investigated. As shown in Figure 4b, the loading amount reached the highest level of 652 mg/g with the immobilization efficiency at 40% when the initial protein concentration was 18 mg/mL, which may be attributed to the large specific surface area and hollow mesoporous structure of the carrier. Furthermore, the conversion of resveratrol increased at the beginning with the increasing protein concentration and then decreased, and the conversion reached a maximum of 98.7% in 2 h as the initial protein concentration was 18 mg/mL. This might be ascribed to a gradual monolayer adsorption of lipase onto the carrier at the beginning, and the excessive lipase would induce agglomeration or the multilayer adsorption, leading to restricted substrate access to the active site of lipase. Therefore, the initial protein concentration of 18 mg/mL was selected for immobilization.

#### Activity and Stability of Free CSL and CSL@HMSS- $C_8$ .

In this study, the activity of free and immobilized CSL were evaluated by the detection of *p*-nitrophenol, which comes from the hydrolysis of *p*-nitrophenyl palmitate (*p*-NPP). The activity of CSL@HMSS- $C_8$  was 7.1-fold greater than that of free CSL, and the specific activity was 2.2 times greater as well (Table S2). The recovery activity of immobilized CSL was 88%. The high activity of CSL@HMSS- $C_8$  laid a good foundation for the efficient preparation of resveratrol esters, and the considerable recovery activity indicated that the CSL@HMSS- $C_8$  has practical value.

The thermal stability is shown in Figure 5; the activity of immobilized CSL decreased less and more slowly than that of the free CSL at both temperatures. Free CSL had lost half of its activity within only 60 min at 60 °C. In contrast, CSL@HMSS- $C_8$  still retained 75.6% of its initial activity after 120 min of heat treatment at 60 °C. This phenomenon was more obvious at higher temperature (80 °C), proving that immobilization can improve the thermal stability of CSL. It was the octyl

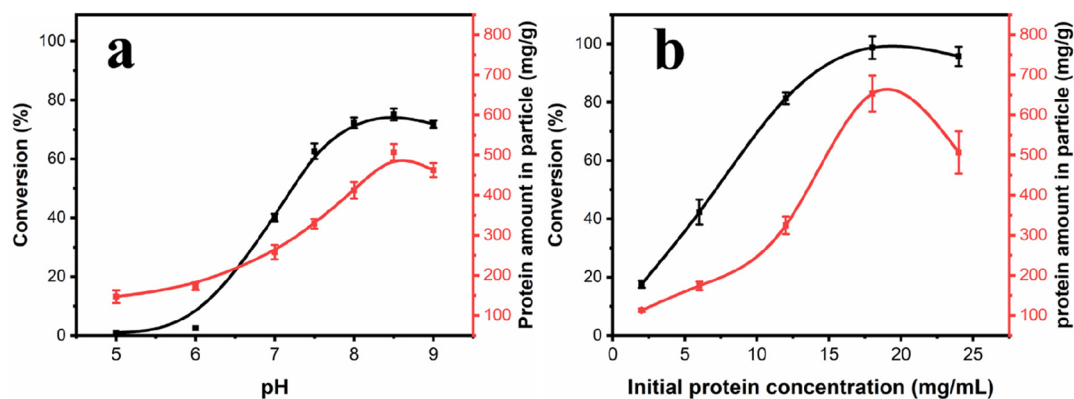


**Figure 4.** Effect of pH (a) and initial protein concentration (b) on immobilized CSL. Reactions were carried out in MTBE (5 mL) containing resveratrol (50 mM), vinyl acetate (750 mM), and CSL@HMSS- $C_8$  (0.1 g) in a shaking incubator (35 °C, 200 rpm).

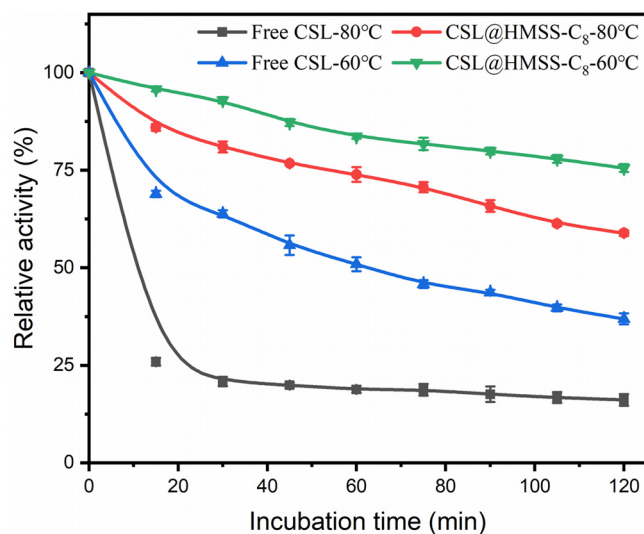


**Figure 5.** Thermal stability of free CSL and CSL@HMSS- $C_8$  at 60 and 80 °C.

group on the carrier that enhanced the hydrophobic interaction between lipase and silica spheres and firmly adsorbed the lipase on the carrier. Meanwhile, the hydroxyl group forms a hydrogen bond with the protein to further stabilize the structure of the lipase and prevent the extensive conformational changes typical of thermal denaturation. The ability to retain enzyme activity at high temperatures affords a number of advantages, such as improved substrate solubility, reaction rate, and conversion, thereby expanding applications of enzymatic synthesis.

#### Acylation of Resveratrol with Different Acyl Donors.

Because lipase-catalyzed acylation is carried out through the formation of a tetrahedral intermediate,<sup>42</sup> the nature of the acyl

donor is essential for the reaction. In acylation, vinyl esters with electron-absorbing properties are generally used as acyl donors because they are easier to react than carboxylic acids. Here, three vinyl esters with different carbon chain lengths were used as acyl donors to react with resveratrol. As shown in Table 2, taking vinyl acetate as acyl donor, the catalytic efficiency (CE, defined as the moles of converted reactants per gram of catalyst per hour) of free CSL was 8 times greater than that of vinyl octyl or vinyl laurate as the acyl donor. The increased steric hindrance accompanied by the long carbon chain might prevent the acyl donor from interacting with lipase to form tetrahedral intermediate, thus leading to a decreased catalytic efficiency. Moreover, the catalytic efficiencies of free CSL and CSL@HMSS- $C_8$  under different acyl donors were compared. The time required for CSL@HMSS- $C_8$ -based catalysis was greatly shortened compared with that of free CSL. Especially when vinyl acetate serves as the acyl donor, the conversion of resveratrol reached 98.8% within 2 h, and the catalytic efficiency was 15 times greater than that of free CSL under the same conditions, which is superior to most values in the current literature (Table S3). The excellent performance of CSL@HMSS- $C_8$  may be due to the hydrophobic interaction and the formation of hydrogen bonds between the carrier and lipase, which protected the lipase from damage to a certain extent. Moreover, because the active center of the lipase is covered by a helical cap-like structure formed by hydrophobic amino acid residues (also known as the “lid”), the outer surface of the lid is hydrophilic while the inner surface is hydrophobic. The alkyl graft enhanced the hydrophobicity of carrier, on which the lid structure of lipase was rearranged, the exposed active sites would facilitate the substrate-lipase proximity to form tetrahedral intermediate. At the same time, the cavity structure in the carrier facilitated the access of the substrates, again promoting the contact between the lipase and the substrate. Overall, the CSL@HMSS- $C_8$  exhibited the highest

**Table 2.** Acylation of Resveratrol with Different Acyl Donors Catalyzed by Free CSL and CSL@HMSS- $C_8$ <sup>a</sup>

| acyl donor                | free CSL |                |                 | CSL@HMSS- $C_8$ |                |                 |
|---------------------------|----------|----------------|-----------------|-----------------|----------------|-----------------|
|                           | time (h) | conversion (%) | CE (mmol/(g·h)) | time (h)        | conversion (%) | CE (mmol/(g·h)) |
| vinyl acetate             | 24       | 81.3           | 0.085           | 2               | 98.8           | 1.235           |
| vinyl <i>n</i> -octanoate | 168      | 67.3           | 0.010           | 36              | 99.5           | 0.069           |
| vinyl laurate             | 168      | 63.4           | 0.009           | 36              | 98.6           | 0.069           |

<sup>a</sup>Reactions were carried out in MTBE (5 mL) containing resveratrol (50 mM), vinyl acetate (750 mM), and lipase (0.1 g) in a shaking incubator (35 °C, 200 rpm).

catalytic activity in the acylation of resveratrol among the reported methods.

Then, the acylated products of resveratrol were identified. Figure 6 displays the HPLC chromatogram of resveratrol

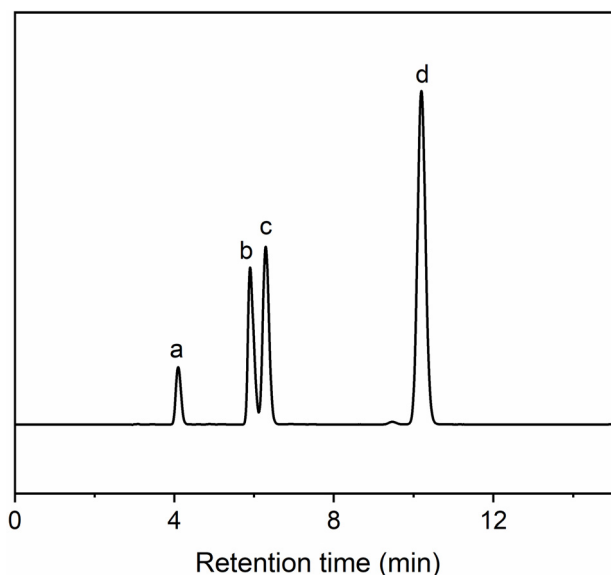


**Figure 6.** HPLC chromatogram of resveratrol esters produced by vinyl acetate as acyl donor. Reaction was carried out in MTBE (5 mL) containing resveratrol (50 mM), vinyl acetate (750 mM), and CSL@HMSS- $C_8$  (0.1 g) in a shaking incubator (35 °C, 200 rpm) for 1 h. (a, resveratrol; b, 4'-O-acetyl-resveratrol; c, 3-O-acetyl-resveratrol; d, 3,5-di-O-acetyl-resveratrol).

acetate; four peaks appeared at the retention times of 4.1, 5.9, 6.3, and 10.2 min. To further identify the structure of resveratrol acetate, the mass spectrometry (MS) patterns of the main products are shown in Figure S1. Intact resveratrol, two monoesters, and one diester were detected at  $m/z$  229, 271, and 313, respectively. The NMR data of the acylated products of resveratrol are listed in Table 3, and the deductive structures are shown in Figure S2. For 4'-O-acetyl-resveratrol and 3,5-di-O-acetyl-resveratrol, H-2 and H-6 had the same chemical shift because of the symmetric molecule structure. However, for 3-O-acetyl-resveratrol, the peak of H-2 and H-6 was split into

**Table 3.**  $^1H$  Chemical Shifts for the Acetylated Compounds

| $^1H$ position | resveratrol      | 4'-O-acetyl-resveratrol | 3-O-acetyl-resveratrol | 3,5-di-O-acetyl-resveratrol |
|----------------|------------------|-------------------------|------------------------|-----------------------------|
| 2              | 6.37 (s)         | 6.43 (s)                | 6.78–6.75 (m)          | 6.81 (d, 7.2 Hz)            |
| 4              | 6.11 (s)         | 6.16 (s)                | 6.73 (s)               | 6.50 (s)                    |
| 6              | 6.37 (s)         | 6.43 (s)                | 6.78–6.75 (m)          | 6.81 (d, 7.2 Hz)            |
| 2'             | 7.39 (d, 5.2 Hz) | 7.61 (d, 5.2 Hz)        | 7.41 (d, 5.2 Hz)       | 7.47 (d, 5.2 Hz)            |
| 3'             | 6.74 (d, 5.2 Hz) | 7.11 (d, 5.2 Hz)        | 6.75 (d, 5.2 Hz)       | 7.08 (d, 5.2 Hz)            |
| 5'             | 6.74 (d, 5.2 Hz) | 7.11 (d, 5.2 Hz)        | 6.75 (d, 5.2 Hz)       | 7.08 (d, 5.2 Hz)            |
| 6'             | 7.39 (d, 5.2 Hz) | 7.61 (d, 5.2 Hz)        | 7.41 (d, 5.2 Hz)       | 7.47 (d, 5.2 Hz)            |
| 3-OH           | 9.16             | 9.27                    |                        |                             |
| 5-OH           | 9.16             | 9.26                    | 9.60                   |                             |
| 4'-OH          | 9.55             |                         | 9.72                   | 5.11                        |

two chemical shifts, indicating that the compound was no longer symmetric as a result of esterification. According to the above results, the products that correspond to the retention time of 4.1, 5.9, 6.3, and 10.2 min were resveratrol, 4'-O-acetyl-resveratrol, 3-O-acetyl-resveratrol, and 3,5-di-O-acetyl-resveratrol, respectively. The esterification position of resveratrol mainly occurred at 4'-OH and 3-OH, and lipase CSL showed a similar substrate selectivity for resveratrol and 3-O-acetyl-resveratrol, further esterizing the 3-O-acetyl-resveratrol to 3,5-di-O-acetyl-resveratrol. Therefore, the regioselectivity of lipase CSL was 3-OH > 4'-OH. As the reaction continues, the main product of resveratrol after complete transformation was 3,5-di-O-acetyl-resveratrol.

**Effect of Reaction Conditions on the Production of Monoesters and Diester.** Immobilized CSL can greatly improve the catalytic efficiency; however, the immobilization process has little influence on the selectivity of lipase. The esterification sites and yield of monoesters and diester by free CSL and CSL@HMSS- $C_8$  were almost unanimous (Figure S3). Considering that the monoesters and diester in the products may possess different biological activities, it is meaningful to control the product by facily regulating the reaction conditions. In the acylation of resveratrol, the reaction temperature is a key parameter. As shown in Figure 7a, the effects of temperature on the product were studied. The yield of diester increased greatly with the increasing temperature, while the output of monoesters increased slightly. This might be ascribed to the fact that the moderately high temperature accelerates the mass transfer between substrates, making the reaction proceed in a positive direction continuously, and the rapidly produced monoesters would be esterified on another hydroxyl group; thus, the main product after resveratrol acylation was diester, but the content of monoesters did not change much.

As shown in Figure 7b, the effects of substrate ratio and reaction time on the conversion of the monoesters and diester were further investigated. The total conversion of resveratrol showed an upward trend with increasing substrate ratio, and the yield of monoesters gradually increased within 30 min. After that, the increased molar ratio would decrease the yield of monoesters gradually, while that of diester increased instead. In addition, when the substrate molar ratio was 1:5, the yield of the monoesters was 38.8%. With the prolonging of reaction time, the monoesters content was nearly unaffected, but the diester content increased further. When the substrate molar ratio was 1:15 or 1:20, the yield of monoesters could be up to 50% in 15 min, and the yield of monoesters reduced to about 20% and diester increased to 80% when reacting for two hours. These results indicate that in the case of a low molar ratio or a short reaction time, the synthesis tends to generate monoesters, and in a high molar ratio or a long-term reaction, diester production is favorable. This phenomenon was attributed to the fact that the hydroxyl groups on resveratrol have not been completely esterified in a short reaction time or low molar ratios. Therefore, not only was the acetylation of resveratrol complete within two hours, but also the content of monoesters and diester in the product could be adjusted by facile control of the substrate molar ratio and reaction time, and the content of diester could be adjusted up to 80%.

**Antioxidant Activity Evaluation of Resveratrol Ester Derivatives.** The ultimate purpose of this work is to improve the biological activity of resveratrol by increasing its lipid solubility, especially the antioxidant activity. Therefore, it is

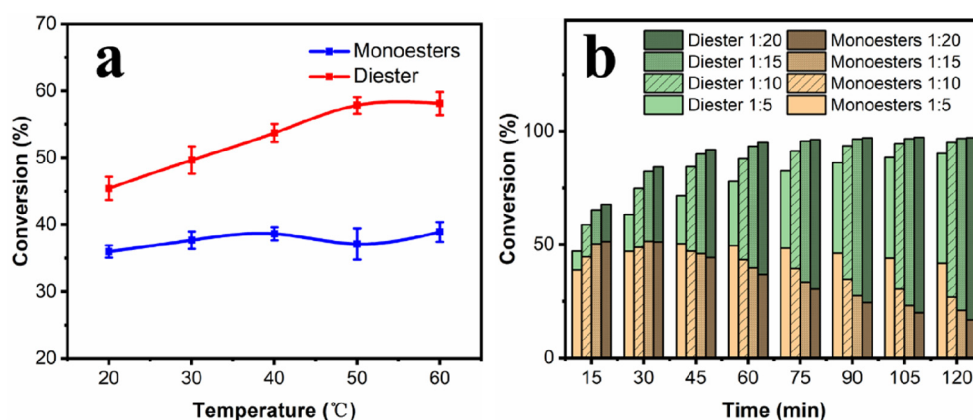


**Figure 7.** Effect of temperature (a) and substrate molar ratio (b) on the reaction conversion. Reactions were carried out in MTBE (5 mL) containing resveratrol (50 mM), vinyl acetate (750 mM), and CSL@HMSS- $C_8$  (0.1 g) in a shaking incubator (35 °C, 200 rpm).

necessary to evaluate the antioxidant properties of its acylated products. The antioxidant effect of resveratrol and the products of monoesters and diester on linseed oil, soybean oil, rapeseed oil, and peanut oil were investigated by measuring the oxidation induction time. Each kind of vegetable oil showed a special oxidative stability index due to their different fatty acid compositions. The oxidation stability index values of linseed oil, soybean oil, rapeseed oil, and peanut oil without any additive were 0.97, 4.49, 5.71, and 6.25 h, respectively. In order to compare the antioxidant properties of resveratrol, monoesters, and diester more clearly, the relative oxidation stability index was introduced (each refined oil without any additive was regarded as 100%). As shown in Figure 8,

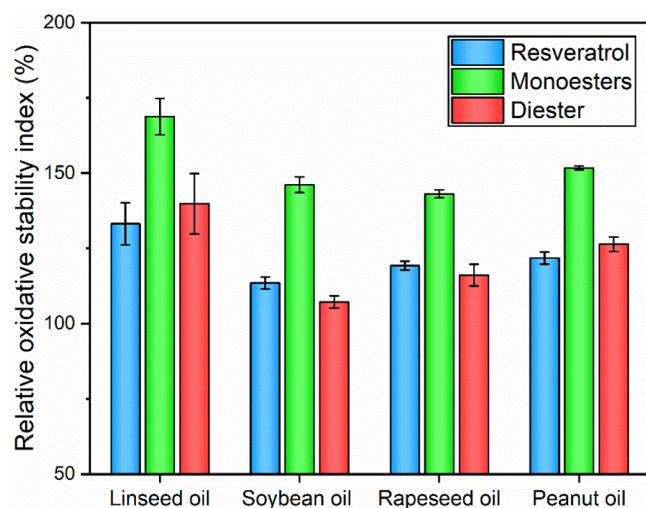


**Figure 8.** Relative oxidation stability index of different vegetable oils containing resveratrol or its acylation products. (The relative oxidation index of each refined oil without any additive was regarded as 100%.)

compared with refined oil, the relative oxidation stability index of linseed oil, soybean oil, rapeseed oil, and peanut oil containing resveratrol increased by 33.2%, 13.5%, 19.3%, and 21.8%, respectively. Surprisingly, the relative oxidation stability index of these vegetable oils containing resveratrol monoesters increased by 68.8%, 46.1%, 43.1%, and 51.8%, respectively. According to the above measurements, the vegetable oil containing resveratrol monoesters was calculated to maintain a relative oxidation stability index greater than that of resveratrol,

by 35.6%, 32.6%, 23.9%, and 30.0%, respectively. This may be ascribed to the poor lipid solubility of resveratrol, which could not be well dispersed in the vegetable oil to exert its antioxidant capacity, while the lipid solubility of the derivatives after esterification was enhanced. However, the refined oil added with resveratrol diester showed a lower relative oxidative stability index than that of resveratrol monoesters, which was close to that of resveratrol. It is acceptable because the antioxidant activity of resveratrol is mainly derived from its phenolic hydroxyl group, which provides hydrogen atoms to react with free radicals so that free radicals are eliminated. As the degree of substitution of the phenolic hydroxyl group increases, the antioxidant activity decreased subsequently. Therefore, the monoester derivatives of resveratrol showed better antioxidant activity than those of resveratrol and diester derivatives, which not only increases lipid solubility but also maintains the antioxidant activity to the maximum extent.

**Recycling of CSL@HMSS- $C_8$ .** The reusability of immobilized enzymes is crucial for practical applications, and the repeated activity of CSL@HMSS- $C_8$  was investigated by transesterification of vinyl acetate and resveratrol. After the completion of each batch of reactions, CSL@HMSS- $C_8$  was separated from the reaction medium by high-speed centrifugation (7656g, 10 min) and then added to the next batch of reactions. As shown in Figure 9, with the recycling of immobilized lipase, the conversion of resveratrol decreased slightly. After 10 cycles, the conversion rate remained as high as 86.3%. The excellent recycling performance of immobilized lipase may be attributed to the HMSS- $C_8$ , which protects the lipase from friction and shear damage during stirring reactions and centrifugal separation. Meanwhile, the hydroxyl groups on HMSS- $C_8$  formed hydrogen bonds with proteins to further stabilize the structure of the lipase and prevent the lipase from denaturing in polar solvents. The cavities and mesopores in HMSS- $C_8$  ensure the mass transfer of the substrate and the separation of the product. Therefore, HMSS- $C_8$  is an ideal support for lipase immobilization and the subsequent catalytic esterification.

In conclusion, the hydrophobic modified hollow mesoporous silica sphere was prepared for the immobilization of lipase CSL, and the immobilized lipase could catalyze the acylation between resveratrol and vinyl ester with different carbon chain lengths efficiently, reaching 98.8% conversion of resveratrol within 2 h. After 10 cycles, the conversion of resveratrol remained up to 86.3%. In addition, the monoesters and diester

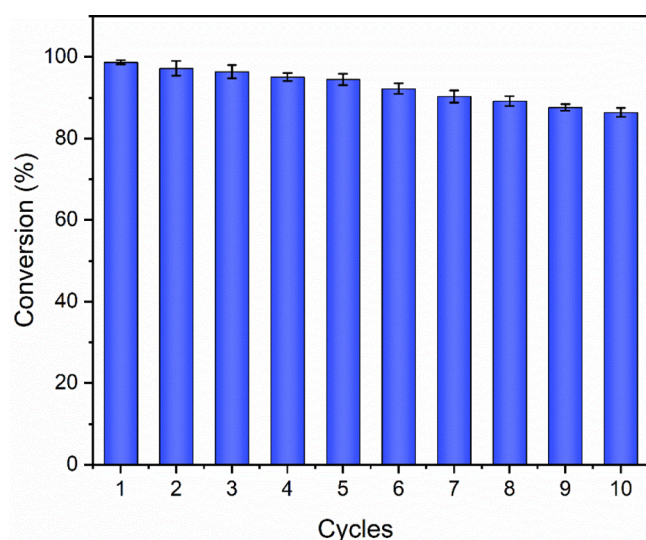


**Figure 9.** Recycling studies on CSL@HMSS-C<sub>8</sub>. Reactions were carried out in MTBE (5 mL) containing resveratrol (50 mM), vinyl acetate (750 mM), and CSL@HMSS-C<sub>8</sub> (0.1 g) in a shaking incubator (35 °C, 200 rpm) for 2 h.

production can be modulated by adjusting the reaction conditions. Monoester derivatives of resveratrol showed better antioxidant activity than those of resveratrol and diester derivatives, which not only increases solubility but also maintains antioxidant activity to the maximum extent. This research provides a new path for extended application of resveratrol in food and pharmaceutical fields.

## ■ ASSOCIATED CONTENT

### SI Supporting Information

The Supporting Information is available free of charge at <https://pubs.acs.org/doi/10.1021/acs.jafc.0c07501>.

Measurement of the immobilized CSL activity and stability; measurement of the loading amount and immobilization efficiency of CSL@HMSS-C<sub>8</sub>; elemental content data of HMSS and HMSS-C<sub>8</sub> and the grafting degree of C<sub>8</sub> (Table S1); comparison of lipase activity and specific activity between free CSL and CSL@HMSS-C<sub>8</sub> and the lipase activity recovery of CSL@HMSS-C<sub>8</sub> (Table S2); comparison between reported enzymatic methods and that in this work for the synthesis of resveratrol ester with vinyl acetate (Table S3); mass spectra of resveratrol acetyl esters (Figure S1); <sup>1</sup>H NMR spectrogram of resveratrol acetyl esters (Figure S2); HPLC chromatogram of resveratrol esters produced by free CSL and immobilized CSL (Figure S3) (PDF)

## ■ AUTHOR INFORMATION

### Corresponding Author

**Ming-Ming Zheng** – Oil Crops Research Institute, Chinese Academy of Agricultural Sciences, Hubei Key Laboratory of Lipid Chemistry and Nutrition, Key Laboratory of Oilseeds Processing, Ministry of Agriculture, Wuhan 430062, China; [orcid.org/0000-0002-4965-2451](https://orcid.org/0000-0002-4965-2451); Email: [zhengmingming@caas.cn](mailto:zhengmingming@caas.cn)

## Authors

**Liu-Jia Xu** – Oil Crops Research Institute, Chinese Academy of Agricultural Sciences, Hubei Key Laboratory of Lipid Chemistry and Nutrition, Key Laboratory of Oilseeds Processing, Ministry of Agriculture, Wuhan 430062, China  
**Tao Yang** – Oil Crops Research Institute, Chinese Academy of Agricultural Sciences, Hubei Key Laboratory of Lipid Chemistry and Nutrition, Key Laboratory of Oilseeds Processing, Ministry of Agriculture, Wuhan 430062, China  
**Jing Wang** – Oil Crops Research Institute, Chinese Academy of Agricultural Sciences, Hubei Key Laboratory of Lipid Chemistry and Nutrition, Key Laboratory of Oilseeds Processing, Ministry of Agriculture, Wuhan 430062, China  
**Feng-Hong Huang** – Oil Crops Research Institute, Chinese Academy of Agricultural Sciences, Hubei Key Laboratory of Lipid Chemistry and Nutrition, Key Laboratory of Oilseeds Processing, Ministry of Agriculture, Wuhan 430062, China; [orcid.org/0000-0003-0654-6947](https://orcid.org/0000-0003-0654-6947)

Complete contact information is available at: <https://pubs.acs.org/doi/10.1021/acs.jafc.0c07501>

## Author Contributions

#L.-J.X. and T.Y. contributed equally to this work.

## Funding

The authors are grateful to the National Natural Science Foundation of China (31972038 and 31671820), the Applied Basic Frontiers Program of Wuhan City (2019020701011474), the Shandong Provincial Key Research and Development Program (2019GHZ031), and the Agricultural Science and Technology Innovation Project of the Chinese Academy of Agricultural Sciences (CAAS-ASTIP-2013-OCRI).

## Notes

The authors declare no competing financial interest.

## ■ REFERENCES

- (1) Park, E. J.; Pezzuto, J. M. The pharmacology of resveratrol in animals and humans. *Biochim. Biophys. Acta, Mol. Basis Dis.* **2015**, *1852*, 1071–1113.
- (2) Donnelly, L. E.; Newton, R.; Kennedy, G. E.; Fenwick, P. S.; Leung, R. H. F.; Ito, K.; Russell, R. E. K.; Barnes, P. J. Anti-inflammatory effects of resveratrol in lung epithelial cells: molecular mechanisms. *Am. J. Physiol.: Lung Cell. Mol. Physiol.* **2004**, *287*, L774.
- (3) Han, G.; Xia, J.; Gao, J.; Inagaki, Y.; Tang, W.; Kokudo, N. Antitumor effects and cellular mechanisms of resveratrol. *Drug Discoveries Ther.* **2015**, *9*, 1–12.
- (4) Carpena, C.; Les, F.; Casedas, G.; Peiro, C.; Fontaine, J.; Chaplin, A.; Mercader, J.; Lopez, V. Resveratrol Anti-Obesity Effects: Rapid Inhibition of Adipocyte Glucose Utilization. *Antioxidants* **2019**, *8*, 74.
- (5) Mokni, M.; Limam, F.; Elkahoui, S.; Amri, M.; Aouani, E. Strong cardioprotective effect of resveratrol, a red wine polyphenol, on isolated rat hearts after ischemia/reperfusion injury. *Arch. Biochem. Biophys.* **2007**, *457*, 1.
- (6) ur Rasheed, M. S.; Tripathi, M. K.; Mishra, A. K.; Shukla, S.; Singh, M. P. Resveratrol Protects from Toxin-Induced Parkinsonism: Plethora of Proofs Hitherto Petty Translational Value. *Mol. Neurobiol.* **2016**, *53*, 2751–2760.
- (7) Bitterman, J. L.; Chung, J. H. Metabolic effects of resveratrol: addressing the controversies. *Cell. Mol. Life Sci.* **2015**, *72*, 1473–1488.
- (8) Smoliga, J. M.; Blanchard, O. Enhancing the Delivery of Resveratrol in Humans: If Low Bioavailability is the Problem, What is the Solution? *Molecules* **2014**, *19*, 17154–17172.
- (9) Walle, T.; Hsieh, F.; DeLegge, M. H.; Oatis, J. E.; Walle, U. K. High absorption but very low bioavailability of oral resveratrol in humans. *Drug Metab. Dispos.* **2004**, *32*, 1377.

- (10) Azzolini, M.; Mattarei, A.; La Spina, M.; Marotta, E.; Zoratti, M.; Paradisi, C.; Biasutto, L. Synthesis and Evaluation as Prodrugs of Hydrophilic Carbamate Ester Analogues of Resveratrol. *Mol. Pharmaceutics* **2015**, *12*, 3441–3454.
- (11) Sawata, Y.; Matsukawa, T.; Doi, S.; Tsunoda, T.; Kotake, Y.; et al. A novel compound, ferulic acid-bound resveratrol, induces the tumor suppressor gene p15 and inhibits the three-dimensional proliferation of colorectal cancer cells. *Mol. Cell. Biochem.* **2019**, *462*, 25–31.
- (12) Oh, W. Y.; Shahidi, F. Lipophilization of Resveratrol and Effects on Antioxidant Activities. *J. Agric. Food Chem.* **2017**, *65*, 8617–8625.
- (13) Kang, S. S.; Cuendet, M.; Endringer, D. C.; Croy, V. L.; Pezzuto, J. M.; Lipton, M. A. Synthesis and biological evaluation of a library of resveratrol analogues as inhibitors of COX-1, COX-2 and NF- $\kappa$ B. *Bioorg. Med. Chem.* **2009**, *17*, 1044–1054.
- (14) Torres, P.; Poveda, A.; Jimenez-Barbero, J. S.; Ballesteros, A.; Plou, F. J. Regioselective lipase-catalyzed synthesis of 3-O-acyl-derivatives of resveratrol and study of their antioxidant properties. *J. Agric. Food Chem.* **2010**, *58*, 807–813.
- (15) Xuejing, Z.; Jie, Z.; Xiaoyun, X.; Yong, Z.; Izhen, L. H. Synthesis of Resveratrol and Resveratrol Trinicotinate. *J. Chin. Pharm. Sci.* **2004**, *1*, 10–13.
- (16) Wang, Z.; Zhang, Y.; Zheng, L.; Cui, X.; Huang, H.; Geng, X.; Xie, X. Regioselective acylation of resveratrol catalyzed by lipase under microwave. *Green Chem. Lett. Rev.* **2018**, *11*, 312–317.
- (17) Dong, Z.; Jiang, M. Y.; Shi, J.; Zheng, M. M.; Huang, F. H. Preparation of Immobilized Lipase Based on Hollow Mesoporous Silica Spheres and Its Application in Ester Synthesis. *Molecules* **2019**, *24*, 395.
- (18) Kidwai, M.; Jain, A.; Sharma, A.; Kuhad, R. C. First time reported enzymatic synthesis of new series of quinoxalines—A green approach. *J. Mol. Catal. B: Enzym.* **2012**, *74*, 236–240.
- (19) Ko, W. C.; Wang, H. J.; Hwang, J. S.; Hsieh, C. W. Efficient hydrolysis of tuna oil by a surfactant-coated lipase in a two-phase system. *J. Agric. Food Chem.* **2006**, *54*, 1849–1853.
- (20) Wang, D. L.; Nag, A.; Lee, G. C.; Shaw, J. F. Factors affecting the resolution of dl-menthol by immobilized lipase-catalyzed esterification in organic solvent. *J. Agric. Food Chem.* **2002**, *50*, 262–265.
- (21) Weitkamp, P.; Weber, N.; Vosmann, K. Lipophilic (hydroxy)-phenylacetates by solvent-free lipase-catalyzed esterification and transesterification in vacuo. *J. Agric. Food Chem.* **2008**, *56*, 5083.
- (22) Köse, z.; Tüter, M.; Aksoy, H. A. E. Immobilized *Candida antarctica* lipase-catalyzed alcoholysis of cotton seed oil in a solvent-free medium. *Bioresour. Technol.* **2002**, *83*, 125–129.
- (23) Kuo, C. H.; Hsiao, F. W.; Chen, J. H.; Hsieh, C. W.; Liu, Y. C.; Shieh, C.-J. Kinetic aspects of ultrasound-accelerated lipase catalyzed acetylation and optimal synthesis of 4'-acetoxyresveratrol. *Ultrason. Sonochem.* **2013**, *20*, 546–552.
- (24) Teng, R. W.; Bui, T. K. A.; Mcmanus, D.; et al. Regioselective acylation of several polyhydroxylated natural compounds by *Candida antarctica* lipase B. *Biocatal. Biotransform.* **2005**, *23*, 109–116.
- (25) Habulin, M.; Krmelj, V.; Knez, Z. Synthesis of oleic acid esters catalyzed by immobilized lipase. *J. Agric. Food Chem.* **1996**, *44* (1), 338–342.
- (26) Bonzom, C.; Schild, L.; Gustafsson, H.; Olsson, L. Feruloyl esterase immobilization in mesoporous silica particles and characterization in hydrolysis and transesterification. *BMC Biochemistry.* **2018**, *19*, 1.
- (27) Nikolic, M.; Srdic, V.; Antov, M. Immobilization of lipase into mesoporous silica particles by physical adsorption. *Biocatal. Biotransform.* **2009**, *27*, 254–262.
- (28) Dong, Z.; Zheng, M. M.; Liu, Z.; Shi, J.; Xiang, X.; Tang, H.; Huang, F. Carbon Nanoparticle-stabilized Pickering Emulsion as a Sustainable and High-performance Interfacial Catalysis Platform for Enzymatic Esterification/Transesterification. *ACS Sustainable Chem. Eng.* **2019**, *7*, 7619–7629.
- (29) Cai, Z.; Wei, Y.; Wu, M.; Guo, Y.; Zhang, H.; et al. Lipase immobilized on layer-by-layer polysaccharide-coated Fe<sub>3</sub>O<sub>4</sub>@SiO<sub>2</sub> microspheres as a reusable biocatalyst for the production of structured lipids. *ACS Sustainable Chem. Eng.* **2019**, *7*, 6685–6695.
- (30) Jung, S.; Park, S. Dual-Surface Functionalization of Metal-Organic Frameworks for Enhancing the Catalytic Activity of *Candida antarctica* Lipase B in Polar Organic Media. *ACS Catal.* **2017**, *7*, 438–442.
- (31) Sun, Q.; Fu, C. W.; Aguila, B.; Perman, J.; Wang, S.; Huang, H. Y.; Xiao, F. S.; Ma, S. Pore Environment Control and Enhanced Performance of Enzymes Infiltrated in Covalent Organic Frameworks. *J. Am. Chem. Soc.* **2018**, *140*, 984–992.
- (32) Teng, Z. G.; Su, X. D.; Zheng, Y. Y.; Sun, J.; Chen, G. T.; Tian, C. C.; Wang, J. D.; Li, H.; Zhao, Y.; Lu, G. M. Mesoporous silica hollow spheres with ordered radial mesochannels by a spontaneous self-transformation approach. *Chem. Mater.* **2013**, *25* (1), 98–105.
- (33) Teng, Z. G.; Han, Y. D.; Li, J.; Yan, F.; Yang, W. S. Preparation of hollow mesoporous silica spheres by a sol-gel/emulsion approach. *Microporous Mesoporous Mater.* **2010**, *127*, 67–72.
- (34) Zheng, M. M.; Mao, L. J.; Huang, F. H.; Xiang, X.; Deng, Q. C.; Feng, Y. Q. A mixed-function-grafted magnetic mesoporous hollow silica microsphere immobilized lipase strategy for ultrafast transesterification in a solvent-free system. *RSC Adv.* **2015**, *5*, 43074–43080.
- (35) Nicolosi, G.; Spatafora, C.; Tringali, C. Chemo-enzymatic preparation of resveratrol derivatives. *J. Mol. Catal. B: Enzym.* **2002**, *16*, 223–229.
- (36) Ozturk, T. K.; Kilinc, A. Immobilization of lipase in organic solvent in the presence of fatty acid additives. *J. Mol. Catal. B: Enzym.* **2010**, *67*, 214–218.
- (37) Zhang, S.; Deng, Q.; Shangguan, H.; Zheng, C.; Shi, J.; Huang, F.; Tang, B. Design and Preparation of Carbon Nitride-Based Amphiphilic Janus N-Doped Carbon/MoS<sub>2</sub> Nanosheets for Interfacial Enzyme Nanoreactor. *ACS Appl. Mater. Interfaces* **2020**, *12*, 12227–12237.
- (38) Thörn, C.; Udatha, D. B. R. K. G.; Zhou, H.; Christakopoulos, P.; Topakas, E.; Olsson, L. Understanding the pH-dependent immobilization efficacy of feruloyl esterase-C on mesoporous silica and its structure–activity changes. *J. Mol. Catal. B: Enzym.* **2013**, *93*, 65–72.
- (39) Ren, M. Y.; Bai, S.; Zhang, D. H.; Sun, Y. pH Memory of Immobilized Lipase for (±)-Menthol Resolution in Ionic Liquid. *J. Agric. Food Chem.* **2008**, *56* (7), 2388–2391.
- (40) Gao, J. K.; Jiang, Y. J.; Lu, S. J.; Han, Z.; Deng, J. J.; Chen, Y. Dopamine-functionalized mesoporous onion-like silica as a new matrix for immobilization of lipase *Candida* sp. 99–125. *Sci. Rep.* **2017**, *7*, 40395.
- (41) Esakkiraj, P.; Antonyraj, C. B.; Meleppat, B.; Ankaiah, D.; Ayyanna, R.; Ahamed, S. I. B.; Arul, V. Molecular characterization and application of lipase from *Bacillus* sp. PU1 and investigation of structural changes based on pH and temperature using MD simulation. *Int. J. Biol. Macromol.* **2017**, *103*, 47–56.
- (42) Gandhi, N. N.; Patil, N. S.; Sawant, S. B.; Joshi, J. B.; Wangikar, P. P.; Mukesh, D. Lipase-Catalyzed Esterification. *Catal. Rev.: Sci. Eng.* **2000**, *42* (4), 439–480.